Supporting Information

Microfluidic-Directed Biomimetic Bulbine-torta-like Microfibers Based on Inhomogeneous Viscosity Rope-coil Effect

Yongshi Guo, [a] Jianhua Yan, [ad] John H. Xin, [b] Lihuan Wang, [a] Xi Yu, [a] Longfei Fan, [a] Peifeng Liu, [c] Hui Yu*[a]

[a] Guangdong-Hong Kong Joint Laboratory for New Textile Materials, School of Textile Materials and Engineering, Wuyi University, Jiangmen, 529020, China

[b] Institute of Textiles & Clothing, The Hong Kong Polytechnic University, Hung Hom, Kowloon, Hong Kong, China

[c] State Key Laboratory of Oncogenes and Related Genes, Shanghai Cancer Institute, Renji Hospital, School of Medicine, Shanghai Jiao Tong University, Shanghai, 200032, China.

Central Laboratory, Renji Hospital, School of Medicine, Shanghai Jiao Tong University, Shanghai, 200127, China.

[d] State Key Laboratory for Modification of Chemical Fibers and Polymer Materials, Donghua University, Shanghai 201620, China

***To whom correspondence should be addressed:**

E-mail:yuhuihui_2000@163.com (Hui Yu)

Tel/fax:+86-750-3296413

Supplemental figures and tables

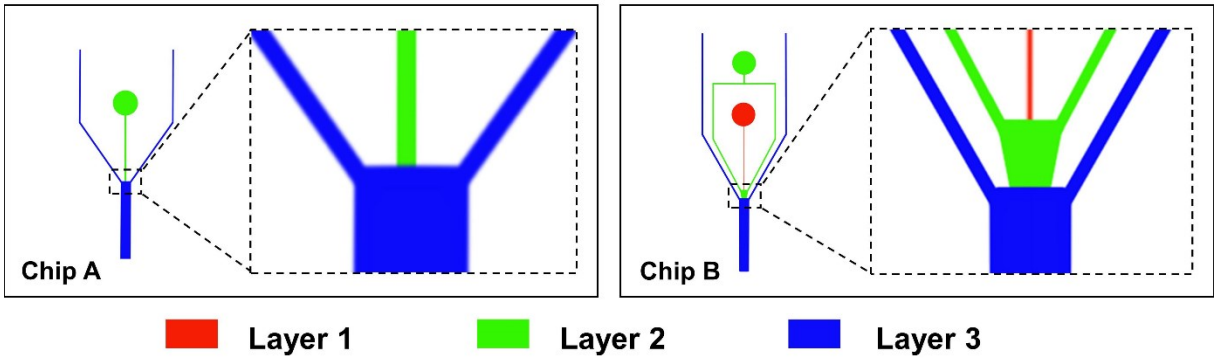

Fig. S1 Two types of chips (Chip A and Chip B) used in experiments. Chip A was used to prepare regular BT microfibers while Chip B was to prepare hollow BT microfibers.

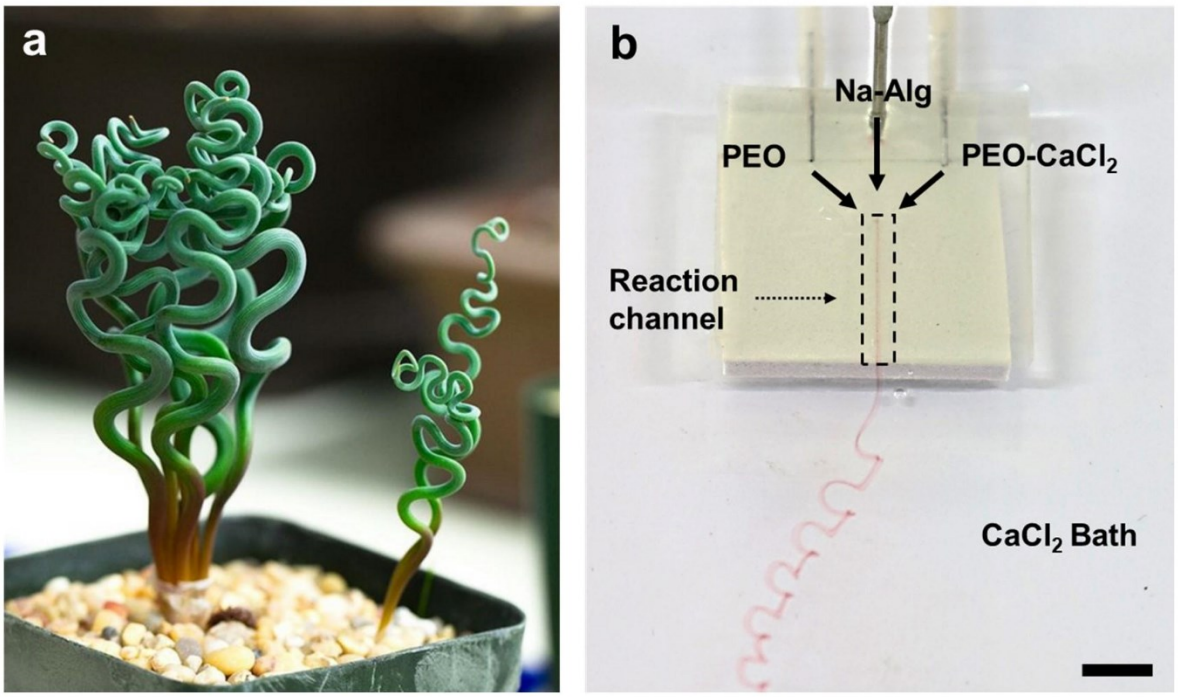

Fig. S2 Inspiration for BT microfibers and their fabrication process: a) *Bulbine torta* (photograph obtained from Internet); b) formation process of BT microfibers. PEO and PEO-$CaCl_2$ solutions were injected into outer-flow channels of microfluidic chip while Na-Alg solution was injected into inner-flow channel. Three fluid phases then merged in reaction channel and formed laminar flow. Finally, fluid was injected into $CaCl_2$ coagulation bath, resulting in formation of atypical helical structure. Scale bar is 2 mm.

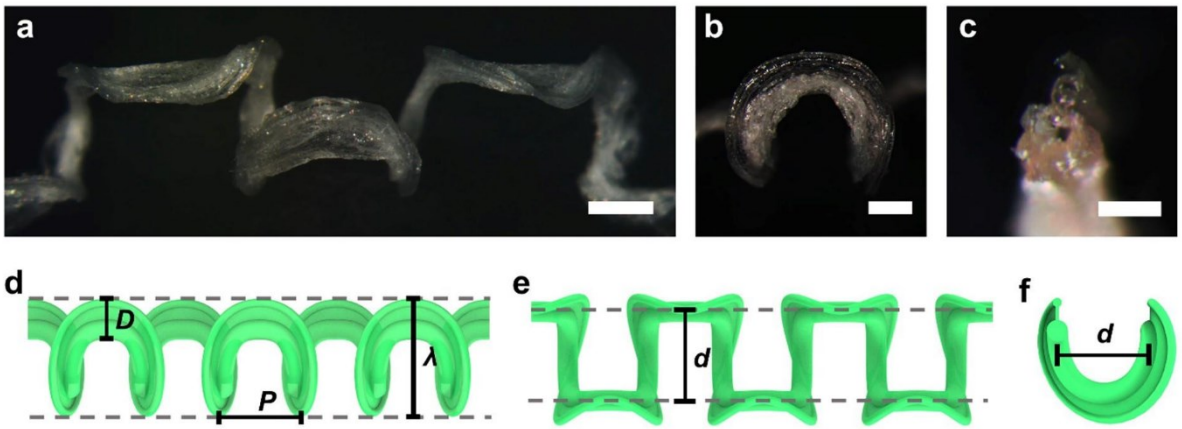

Fig. S3 a) Asana microscope image of BT microfiber with 3D structure; scale bar is 500 μm. b) Asana microscope image of surface morphology of BT microfiber; scale bar is 300 μm. c) Asana microscope image of BT microfiber profile shape; scale bar is 100 μm. d-f) Structural parameters of BT microfibers, including diameter (D), pitch (P), wavelength (λ)), and depth (d).

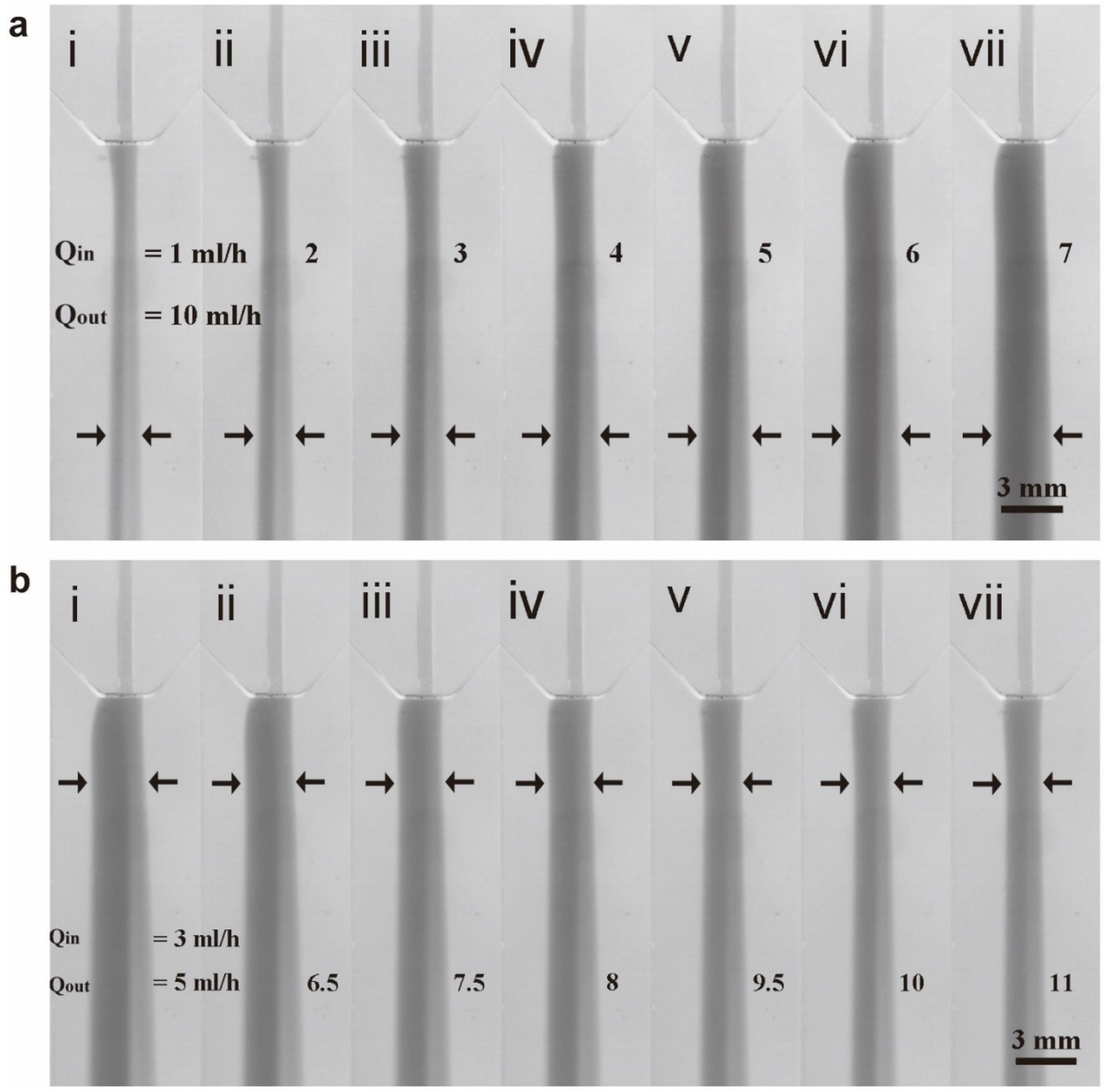

Fig. S4 Amount of alginate solution in microchip was changed by varying internal and external phase velocities. a) Effect of external phase velocity on intermediate prepolymer. b) Effect of internal-phase flow rate on intermediate prepolymer. Bar is 3 mm.

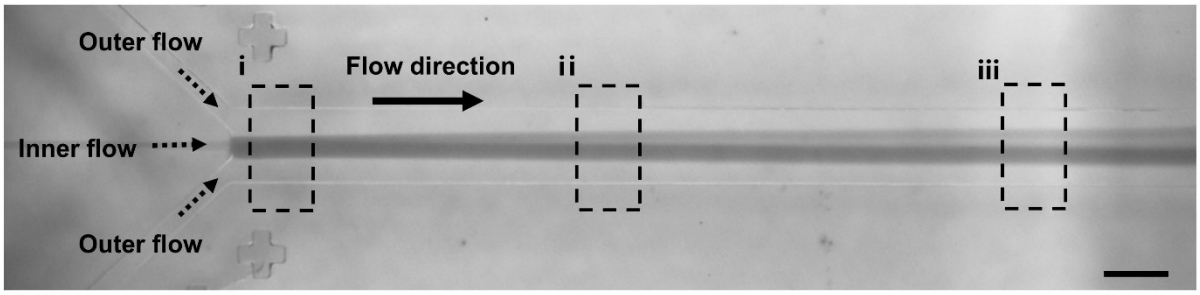

Fig. S5 The flow change process of microfluidics in microchannel photographed by high speed camera. (i)–(iii) show changes in internal-phase fluid in channel, which exhibits dumbbell-like shape. Bar is 1 mm.

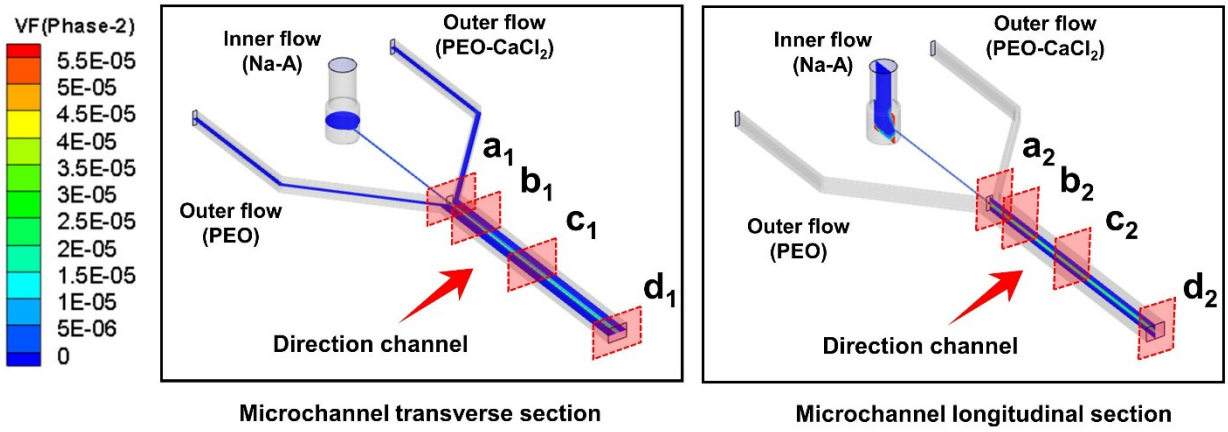

Fig. S6 Volume proportional coefficient distribution of phase fluid in microchannel profile; the color bar is the volume factor, indicating the volume proportion coefficient of the alginate phase, the red area means of the most alginate volume proportion, while the blue area means of the least.

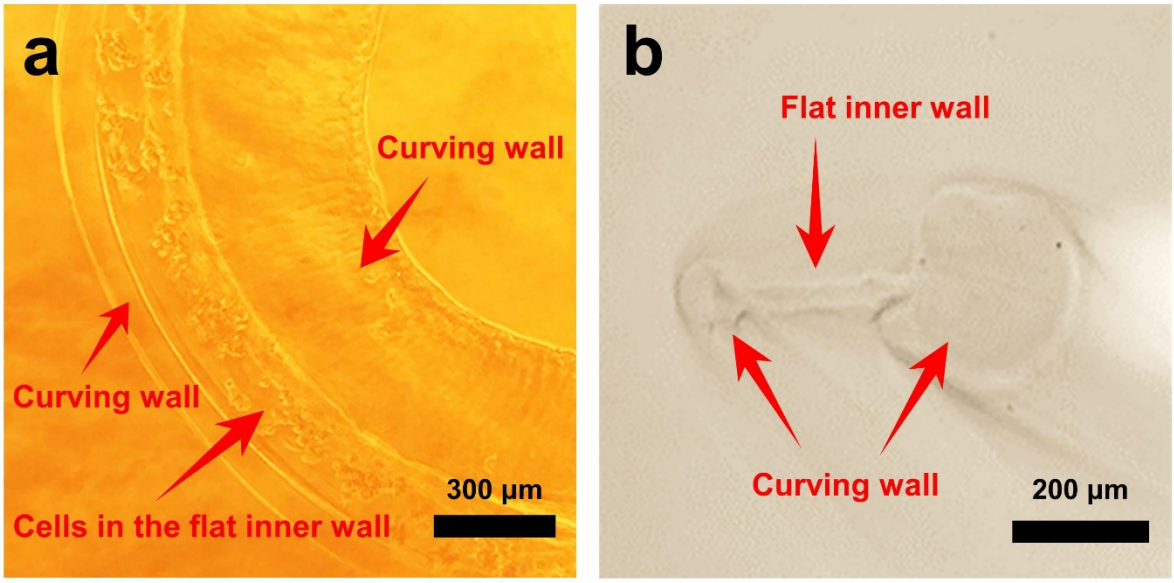

Fig. S7 a) The cells grow on the flat inner wall of the dumbbell-shaped BT microfiber. b) A cross section of the dumbbell-shaped BT microfiber consists of curving wall and a flat inner wall.

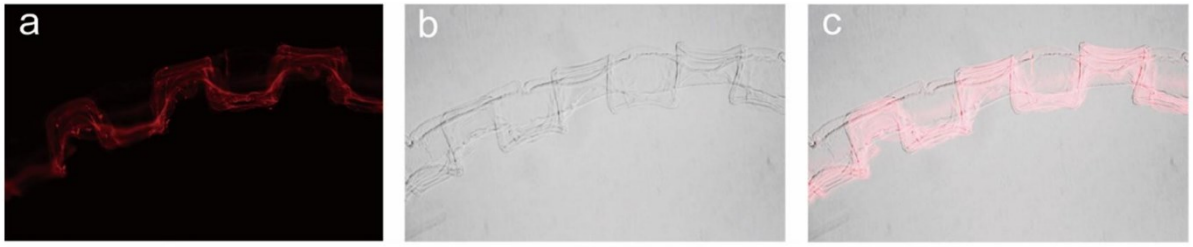

Fig. S8 2D single-hollow microfibers. a) Microscopy images of microfibers containing fluorescent polystyrene nanoparticles. b) Brightfield images of microfibers. c) Composite of brightfield and fluorescence images of microfibers

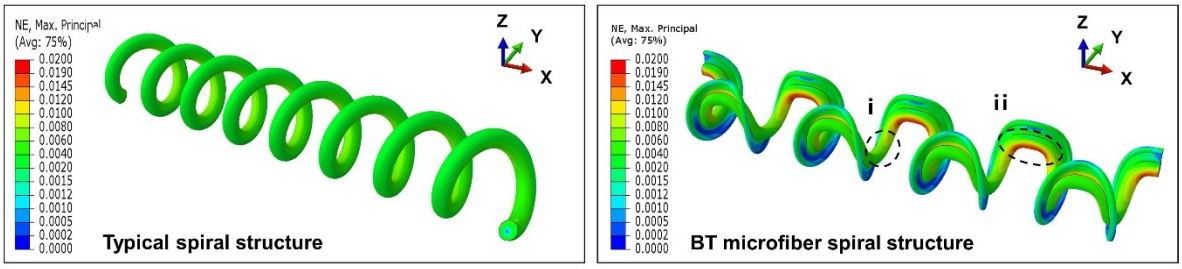

Fig. S9 The element method was used to analyze strain characteristics of typical and BT microfiber spiral structure microfiber. The strain distribution of typical helical structure is uniform. The strain distribution of BT microfiber helical structure is not uniform: i) maximum strain position of BT microfiber; ⅱ） minimum stress concentration of ultrafine fiber.

Table S1. Parameters for synthesis of BT microfibers

Fiber type	Outer flow	Inner flow	Core flow
BT microfibers	5–11 mL h^{-1}	1–7 mL h^{-1}	
Hollow BT microfibers	2.5–15 mL h^{-1}	0.5–3.5 mL h^{-1}	0.5–3.5 mL h^{-1}

Table S2. Specifications of different types of chips, including orifice width and channel height of each layer on PDMS slice

Chip type	Layer 1 (orifice width/channel height)	Layer 2 (orifice width/channel height)	Layer 3 (orifice width/channel height)
A		88/66 μm	950/720 μm
B	75/54 μm	250/424 μm	950/1432 μm

Table S3. Summary of available methods used to measure beatings of cardiomyocytes

Available methods	Advantages	Disadvantages	References
Atomic force microscopy detection	reflecting stress-strain relation directly, response time less than 1ms	damaging the tested sample, time-consuming, unable to test the strain in the x-y plane	(1) (2)
Cell drum evaluation	recording the stress-strain relation for long stretches, test operation in comfortable surroundings	high production cost, low testing accuracy, disposable items	(3) (4)
Traction force microscopy detection	reflecting stress change in one cycle, obtaining stress distribution on any part, non-contact in situ testing	unable to test the vertical shrinkage force, showing a non-continuous record, low testing accuracy	(5) (6)
Calcium imaging measurement	efficient testing with numerous samples at one time	damaging the tested sample, an indirect way to reflecting stress change	(7) (8)
Micropost arrays measurement	recording three-dimensional contractility	unable to obtain the contractility in real-time, damaging cytoskeleton	(9)
Electrochemical impedance measurement	recording the stress-strain relation for long stretches in real-time	an indirect way to reflecting the stress change with cell index	(10)
Mechanical strain sensor based on BT microfibers	reflecting continuous stress-strain relation directly with high sensitivity, non-contact testing	unable to record the vertical shrinkage force	Our work

References:

(1) M. Pesl, J. Pribyl, I. Acimovic, A. Vilotic, S. Jelinkova, A. Salykin, Biosens. Bioelectron.,2016, 85, 751-757.

(2) J. Park, J. Ryu, S. K. Choi, E. Seo, J. M. Cha, S. Ryu, S. H. Lee, Anal. Chem. Anal. Chem., 2005, 77, 6571-6580.

(3) J. Trzewik, A. Artmann-Temiz, P. Linder, T. Demirci, I. Digel, G. Artmann, Ann. Biomed. Eng., 2004, 32,1243-1251.

(4) M. Goßmann, R. Frotscher, P. Linder, S. Neumann, R. Bayer, M. Epple, G. M. Cell. Physiol. Biochem., 2016, 38, 1182-1198.

(5) J. G. Jacot, A. D. Mcculloch, J. H. Omens, Biophys. J., 2008, 95, 3479-3487.

(6) A. Marinković, J. D. Mih, J. A. Park, F. Liu, D. J. Tschumperlin, Am. J. Physiol-Lung C.,

2012, 303, 169-180.

(7) N. L. Francis, N. K. Bennett, A. Halikere, Z. P. Pang, P. V. Moghe, ACS Biomater. Sci. Eng., 2016, 2, 156.

(8) T. Boudou, W. R. Legant, A. Mu, M. A. Borochin, N. Thavandiran, M. Radisic, C. S. Chen, Tissue Eng., Part A, 2012, 18, 910-919.

(9) K. M. Beussman, M. L. Rodriguez, A. Leonard, N. Taparia, C. R. Thompson, N. J. Sniadecki, Methods, 2016, 94, 43-50.

(10) J. Wegener, S. Zink, P. Rösen, H. J. Galla, Pflügers Archiv., 1999, 437, 925-934.